

Inhibition of Dystrophin Breakdown and Endothelial Nitric-Oxide Synthase Uncoupling Accounts for Cytoprotection by 3-[2-[4-(3-Chloro-2-methylphenyl)-1-piperazinyl]ethyl]-5,6-dimethoxy-1-(4-imidazolylmethyl)-1*H*-indazole Dihydrochloride 3.5 Hydrate (DY-9760e) in Left Ventricular Hypertrophied Mice

Feng Han, Ying-Mei Lu, Hideyuki Hasegawa, Hiroshi Kanai, Erika Hachimura, Yasufumi Shirasaki, and Kohji Fukunaga

Institute of Pharmacology, Toxicology, and Biochemical Pharmaceutics, Zhejiang University, Hangzhou, China (F.H.); Department of Pharmacology, Graduate School of Pharmaceutical Sciences, Tohoku University, Sendai, Japan (Y.-M.L., E.H., K.F.); Graduate School of Biomedical Engineering, Tohoku University, Sendai, Japan (H.H.); Graduate School of Engineering, Tohoku University, Sendai, Japan (H.K.); and Daiichi-Sankyo Co., Ltd., Tokyo, Japan (Y.S.)

Received September 15, 2009; accepted November 2, 2009

ABSTRACT

Using a heart ischemia/reperfusion model in rats, we recently demonstrated that 3-[2-[4-(3-chloro-2-methylphenyl)-1-piperazinyl]ethyl]-5,6-dimethoxy-1-(4-imidazolylmethyl)-1*H*-indazole dihydrochloride 3.5 hydrate (DY-9760e), a calmodulin inhibitor, is a cardioprotective drug. Here, we examined cardioprotective mechanisms of DY-9760e in hypertrophy and heart failure using a mouse transverse aortic constriction (TAC) model. Mice were subjected to TAC and 2 weeks later they were administered DY-9760e for another 6 weeks (at 10 or 20 mg/kg/day p.o.). Chronic administration inhibited TAC-induced increased heart-to-body weight ratio dose-dependently. Consistent with inhibition of hypertrophy, fraction shortening, an indicator of heart contractile function, assessed by echocardiography was completely restored by DY-9760e (20 mg/kg/day) administration. Inhibition of TAC-induced atrial natriuretic peptide (ANP) up-regulation further confirmed an antihypertrophic effect of DY-9760e. It is note-

worthy that we found that breakdown of dystrophin and spectrin by calpain was associated with heart failure in TAC mice. Caveolin-3 breakdown was closely associated with endothelial nitric-oxide synthase (eNOS) dissociation from the plasma membrane and its subsequent uncoupling. Uncoupled monomeric eNOS formation was associated with increased protein tyrosine nitration, suggesting peroxynitrite production and NO and superoxide formation. It is important to note that 6 weeks of DY-9760e treatment significantly blocked hypertrophic responses, such as increased heart weight and ANP induction. Overall, we show that inhibition of both dystrophin/spectrin breakdown and uncoupling of eNOS probably underlies the cardioprotective mechanisms of DY-9760e. The observed protection of sarcolemmal proteins and eNOS by DY-9760e during pressure overload suggests a novel therapeutic strategy to rescue the heart from hypertrophy-induced failure.

Cardiac hypertrophy is an adaptive response to prolonged increases in hemodynamic pressure overload and humoral stresses. Although this compensatory process is initially a physiological event to reduce wall stress and oxygen con-

sumption, progressive left ventricular (LV) hypertrophy significantly increases the risk of developing heart failure and sudden death in humans (Levy et al., 1996; Haider et al., 1998; Brown et al., 2000; Meijs et al., 2007). During continuous pressure overload, degradation of sarcolemma and caveolae components, including dystrophin, spectrin, and caveolin-3, in cardiomyocytes triggers cardiomyocyte injury (Weber, 1989; Jugdutt, 2003; Spinale, 2007).

Dystrophin, a 430-kDa rod-shaped protein, is a component of the sarcolemma cytoskeleton in both cardiac and skeletal

This work was supported in part by the Ministry of Education, Science, Sports and Culture of Japan [Grant 19390150] (to K.F.); and by the Uehara Memorial Foundation (to Y.-M.L.) and the Smoking Research Foundation (to K.F.).

F.H. and Y.-M.L. contributed equally to this work.

Article, publication date, and citation information can be found at <http://jpet.aspetjournals.org>.

doi:10.1124/jpet.109.161646.

ABBREVIATIONS: LV, left ventricle; eNOS, endothelial nitric-oxide synthase; CaM, calmodulin; ET, endothelin; DY-9836, 3-(2-(4-(3-chloro-2-methylphenyl)-1-piperazinyl)ethyl)-5,6-dimethoxyindazole; DY-9760e, 3-[2-[4-(3-chloro-2-methylphenyl)-1-piperazinyl]ethyl]-5,6-dimethoxy-1-(4-imidazolylmethyl)-1*H*-indazole dihydrochloride 3.5 hydrate; TAC, transverse aortic constriction; PO, pressure overload; HW, heart weight; BW, body weight; LVEDD, left ventricle end-diastolic diameter; LVESD, left ventricle end-systolic diameter; FS, fraction shortening; PCR, polymerase chain reaction; ANP, atrial natriuretic peptide; PBS, phosphate-buffered saline; BH4, tetrahydrobiopterin.

muscle. Dystrophin is attached to the β -subunit of dystroglycan, a member of a complex of dystrophin-associated glycoproteins. Dystrophins are also associated with other cytoskeletal elements, such as spectrin, through filamentous actin, thereby supporting the submembranous cytoskeletal structure to maintain heart function. Thus, disruption of myocardial dystrophin is a critical event in progression to advanced heart failure (Toyo-oka et al., 2004). Both calpains 1 and 2 account for degradation of dystrophin (Yoshida et al., 2003) and spectrin (Saido et al., 1994).

Caveolin-3 is a component of caveolae in cardiac and skeletal muscles. Caveolin-3 is localized to the sarcolemma and functions in formation of caveolae membranes, serving as a scaffolding protein to interact with and organize lipid and protein constituents, including endothelial nitric-oxide synthase (eNOS), in caveolae. As in endothelial cells, eNOS is targeted to sarcolemmal caveolae through both post-translational myristoylation and later palmitoylation in cardiomyocytes. Caveolin-3 binds to eNOS in caveolae, thereby inhibiting its NO-generating activity. When Ca^{2+} is mobilized into cardiomyocytes through stimulation of calcium channels or GTP-binding protein-coupled receptors localized in caveolae, eNOS is efficiently activated by Ca^{2+} /calmodulin (CaM) (Feron et al., 1996).

We have documented that prolonged exposure of cultured cardiomyocytes to endothelin (ET)-1 causes biphasic changes in dystrophin levels (Lu et al., 2007). We subsequently found that dystrophin levels were markedly elevated during the first 48 h of ET-1 exposure, whereas dystrophin was significantly degraded after 96 h of ET-1 treatment, resulting in instability of sarcolemmal structures, dissociation of caveolin-3 and eNOS from caveolae and eNOS uncoupling, and ultimately apoptosis (Lu et al., 2009a). These *in vitro* studies prompted us to seek novel cardioprotective drugs to prevent dystrophin breakdown and eNOS dysregulation.

We have found that the novel calmodulin antagonist DY-9760e can protect the heart from ischemic/reperfusion injury (Hashimoto et al., 2005) and that its active metabolite DY-9836 prevents phenylephrine-induced injury to cultured cardiomyocytes (Lu et al., 2009a). It is more important that DY-9836 treatment totally inhibited aberrant NO production and superoxide generation by uncoupled eNOS after phenylephrine treatment of these cells (Lu et al., 2009a). We also found that DY-9760e treatment of cultured cardiomyocytes prevents ET-1-induced hypertrophy (Lu et al., 2009b). However, potential antihypertrophic and cardioprotective effects of DY-9760e had not been tested *in vivo* on pressure overload-induced hypertrophy.

Here, we used a mouse heart failure model induced by transverse aortic constriction (TAC)-induced hypertrophy to analyze potential antihypertrophy and cardioprotective effects of DY-9760e *in vivo*. DY-9760e markedly inhibited TAC-induced cardiac hypertrophy with concomitant restoration of contractile function. Our findings strongly suggest that protection of dystrophin and spectrin from calpain-induced degradation as well as inhibition of eNOS uncoupling probably mediates these cardioprotective effects *in vivo*.

Materials and Methods

Animals. Adult male DDY mice weighing 35 to 40 g were obtained from Nippon SLC (Hamamatsu, Japan). Ten-week-old males were

acclimated to the local environment for 1 week, which included housing in polypropylene cages at $23 \pm 1^\circ\text{C}$ in a humidity-controlled environment maintained on a 12-h light/dark schedule (lights on 8:00 AM–8:00 PM). Mice were provided food and water *ad libitum*. Animal experiments were in accordance with the Guide for the Care and Use of Laboratory Animals at Tohoku University. The Medical Experimental Animal Administrative Committee of Tohoku University approved all experiments. All efforts were made to minimize animal suffering and reduce the number of animals used.

Surgical Procedures and Drug Treatment. Transverse aortic constriction (TAC) was performed on males as described previously (Hu et al., 2003). After acclimatization for 7 days, animals were anesthetized with tribromoethanol (0.25–0.3 g/kg *i.p.*). The chest cavity was opened with scissors by a small incision at the level of the second intercostal space. After isolating the aortic arch, a 6-0 silk suture was placed around the aorta with a 27-gauge needle. The needle was immediately removed to produce an aorta with a stenotic lumen. The chest cavity was then closed with one 6-0 nylon suture, during which negative pressure in the thorax was re-established by removing air with a polyethylene-50 chest tube attached to a syringe. Sham-operated animals, which underwent surgery without the final tightening of the constrictive suture, served as controls.

After 2 weeks of TAC or sham surgery, mice were randomly divided into five groups: 1) sham receiving vehicle (0.5% methyl cellulose; $n = 6$), 2) sham receiving DY-9760e at 20 mg/kg ($n = 6$), 3) a pressure overload (PO) group receiving vehicle ($n = 6$), 4) a PO group receiving DY-9760e at 10 mg/kg ($n = 6$), and 5) a PO group receiving DY-9760e at 20 mg/kg ($n = 6$). Mice were orally administered vehicle or DY-9760e daily for another 6 weeks, as indicated.

Measurement of Cardiac Hypertrophy. After 6 weeks of DY-9760e or vehicle administration, animals were subjected to terminal surgery. Mice were weighed and anesthetized with tribromoethanol (0.25–0.3 g/kg *i.p.*). The thoracic cavity was opened, and hearts were immediately harvested and weighed. Cardiac indices, expressed as the ratio of heart (in milligrams) to body (in grams) weight (HW/BW), were used to estimate the degree of cardiac hypertrophy.

Transthoracic Echocardiography. Noninvasive echocardiographic measurements were performed using ultrasonic diagnostic equipment (SSD-6500; Aloka, Tokyo, Japan). In motion-mode images obtained using a 10-Hz linear type ultrasonic probe (UST-5545; Aloka), the following parameters, including LV end-diastolic diameter (LVEDD) and LV end-systolic diameter (LVESD), were used to calculate fraction shortening (FS), as follows: $\%FS = (LVEDD - LVESD)/LVEDD \times 100$. Animals ($n = 4$ in each group) were subjected to echocardiographic analyses after sham operation or TAC at 8 weeks with or without DY-9760e administration.

Reverse Transcription-Polymerase Chain Reaction. Cardiac gene expression was analyzed by reverse transcription-PCR. Total RNA was extracted from heart after 8 weeks of TAC using TRIzol Reagent (Invitrogen, Carlsbad, CA). Two micrograms of total RNA was reverse-transcribed using the Reverse Transcription System (Promega, Madison, WI) according to the manufacturer's protocol. Primer sequences for ANP were as follows: 5'-GTCCAACACAGATCTGATGG-3' and 5'-GATTTGGCTGTTATCTTCGG-3', generating a 377-base pair product. Primer sequences for β -actin were as follows: 5'-CGTCCACCCGCGAGTACAAC-3' and 5'-TCCTTCTGACCCATACCCAC-3', generating a 220-base pair product. PCR amplification was performed using the GeneAmp PCR system 9700 (Applied Biosystems Japan, Chiba, Japan). PCR conditions (ANP: 26 cycles of 94°C for 30 s, 53°C for 30 s, and 72°C for 30 s; brain natriuretic peptide β -actin: 30 cycles of 94°C for 30 s, 55°C for 30 s, and 72°C for 30 s) were determined within the linear amplification range. After separation of PCR products on a 2% agarose gel containing ethidium bromide, products were quantified using an imaging analyzer (ChemiDoc XRS; Bio-Rad Laboratories, Hercules, CA), and expression levels were normalized to those of β -actin.

Western Blot Analysis. All animals were sacrificed after 6 weeks of drug administration. After weighing the heart, the left ventricle

was isolated from each heart ($n = 6$) and stored at -80°C until immunoblotting analyses were performed as described previously (Lu et al., 2007). In brief, equal amounts of protein were separated on 7.5 to 10% SDS-polyacrylamide gel electrophoresis gels and transferred to polyvinylidene difluoride membranes (Millipore, Billerica, MA). Blots were then stained with 0.1% Ponceau S solution to visualize protein bands and confirm equal protein loading among groups. After blocking in 5% nonfat milk, blots were incubated overnight at 4°C with antibodies against dystrophin (mouse monoclonal antibody, 1:1000; Millipore Bioscience Research Reagents, Temecula, CA), spectrin, caveolin-3, eNOS, and nitrotyrosine (rabbit polyclonal antibody, 1:500; Hashimoto et al., 2005; Lu et al., 2009a). Immunoreactive proteins on membranes were visualized with an enhanced chemiluminescence (ECL) detection system (GE Healthcare, Little Chalfont, Buckinghamshire, UK). Images were scanned and analyzed semiquantitatively using Image (National Institutes of Health, Bethesda, MD) and Image Gauge software (Fujifilm, Tokyo, Japan).

Immunohistochemistry. For immunohistochemical studies, an additional three mice in each experimental condition were anesthetized with pentobarbital and perfused via the ascending aorta with 0.1 M phosphate-buffered saline, pH 7.4, until the outflow became clear followed by 0.1 M phosphate buffer, pH 7.4, containing 4% paraformaldehyde for 15 min. The left ventricle was removed and postfixed in the same solution for 24 h at 4°C and then sliced at 35 μm using a Vibratome sectioning system (Dosaka EM Co. Ltd., Kyoto, Japan). Sections were incubated at room temperature with 0.01% Triton X-100 in phosphate-buffered saline for 30 min and for another hour in 3% bovine serum albumin in phosphate-buffered saline. For immunolabeling, slices were probed with anti-dystrophin antibody (1:500) overnight at 4°C . After washing, sections were incubated with biotinylated anti-rabbit IgG (1:5000) in TNB buffer (ECL detection system) for 1 h, followed by streptavidin-horseradish peroxidase (1:5000) labeling for 2 h. Sections were then stained with tetramethylrhodamine tyramide for 10 min using the TSA-Direct kit (PerkinElmer Life and Analytical Sciences, Boston, MA). Immunofluorescent images were acquired using a confocal laser scanning microscope (TCS SP; Leica Microsystems, Inc., Deerfield, IL).

Statistical Analyses. All values are expressed as means \pm S.E.M. Multiple comparisons between experimental groups were made by analysis of variance followed by Dunnett's test. $P < 0.05$ was considered significant.

Results

Inhibitory Effect of DY-9760e on Pressure Overload-Induced Myocardial Hypertrophy in Vivo and Echocardiography Analysis. After 2 weeks of TAC, the heart was slightly enlarged and the wall of ventricle was thickened (Fig. 1A). After 8 weeks of TAC, the ventricular cavity was larger than that seen at 2 weeks. DY-9760e administration (10 or 20 mg/kg orally) for 6 weeks beginning after the first 2 weeks of TAC dose-dependently inhibited heart weight increases, as indicated by the HW/BW ratio, and decreased the size of the left ventricular cavity (Fig. 1B), suggesting that DY-9760e inhibits TAC-induced hypertrophy in vivo.

Next, we used echocardiography to determine whether inhibition of hypertrophy is accompanied by functional recovery of heart contraction. After 8 weeks of TAC, two-dimensional imaging using LV echocardiography showed a significant increase both in LVEDD and LVESD in animals not treated with DY-9760e. By contrast, animals administered DY-9760e (20 mg/kg) showed values comparable with the sham-operated group (Fig. 1C). TAC also resulted in a significant decrease in FS% compared with the sham group in untreated animals. However, this impairment was rescued by 6 weeks of DY-9760e treatment (20 mg/kg) beginning after 2 weeks of TAC (Fig. 1C).

Inhibition of TAC-Induced ANP Expression by DY-9760e Administration. We next confirmed antihypertrophic action of DY-9760e in vivo by measuring ANP mRNA levels in the LV. Although DY-9760e treatment had no effect on baseline ANP expression in sham-operated animals, TAC-induced ANP up-regulation was totally blocked by DY-9760e (20 mg/kg) treatment (Fig. 2).

Inhibitory Effect of DY-9760e on TAC-Induced Degeneration of Dystrophin. We showed previously that DY-9760e treatment inhibits dystrophin breakdown seen in cultured cardiomyocytes after prolonged ET-1 treatment (Lu et al., 2007). Therefore, we evaluated dystrophin levels in LV after TAC in vivo using immunohistochemical analyses of LV cardiomyocytes at 2, 4, and 8 weeks after TAC surgery (Fig. 3A). Compared with strong dystrophin immunoreactivity seen in the plasma membrane of sham-operated animals, membrane dystrophin immunoreactivity in experimental animals was weak and accompanied by increased cardiomyocyte size during the entire period after TAC surgery. Notably, cytoplasmic dystrophin immunoreactivity was weak in cardiomyocytes at 2 and 4 weeks but strong in some cells by 8 weeks (Fig. 3A). We then tested the effect of DY-9760e treatment on dystrophin levels by Western blotting using LV extracts prepared after 8 weeks of TAC. As shown in Fig. 3B, TAC alone markedly reduced dystrophin levels ($50 \pm 3\%$ of the sham group), whereas DY-9760e treatment (20 mg/kg) blocked TAC-induced dystrophin breakdown ($75 \pm 3\%$ of sham group; $p < 0.01$ versus the PO group) (Fig. 3B). These findings indicate that inhibition of dystrophin breakdown by DY-9760e treatment could protect cardiomyocytes in conditions of heart failure.

Effects of DY-9760e on TAC-Induced Spectrin and Caveolin-3 Breakdown. To confirm that TAC-induced dystrophin breakdown is mediated by calpain activity, we investigated calpain activity by assessing a specific, calpain-dependent 150-kDa spectrin breakdown product. As expected, after 8 weeks of TAC, levels of full-length, 240-kDa spectrin were significantly reduced in the absence of DY-9760e (Fig. 4, A and B). These levels recovered dose-dependently after DY-9760e treatment. Inversely, levels of the TAC-induced 150-kDa breakdown product were markedly increased by 270% ($p < 0.05$) and reduced dose-dependently by DY-9760e treatment (Fig. 4, A and C).

Caveolin-3 breakdown by phenylephrine-induced hypertrophy is associated with injury in cultured cardiomyocytes (Lu et al., 2009a). As expected, we observed significant TAC-induced caveolin-3 breakdown in the LV compared with sham-operated animals. Significantly, DY-9760e (20 mg/kg) treatment strongly inhibited this effect (Fig. 4, D and E), suggesting that dystrophin breakdown is accompanied with breakdown of spectrin and caveolin-3.

TAC-Induced eNOS Redistribution after Transverse Aortic Constriction. Because eNOS is localized to caveolae through caveolin-3 in cardiomyocytes (Michel and Feron, 1997), we asked whether dystrophin and caveolin-3 breakdown triggers eNOS dissociation from caveolae. Although total eNOS protein levels in LV extracts remained unchanged in TAC versus sham-operated animals (Fig. 5A), membrane-associated eNOS levels were markedly reduced by TAC, whereas DY-9760e treatment dose-dependently restored plasma membrane eNOS levels (Fig. 5B). We hypothesized that caveolin-3 breakdown in caveolae and concomitant eNOS dissociation from the plasma membrane might

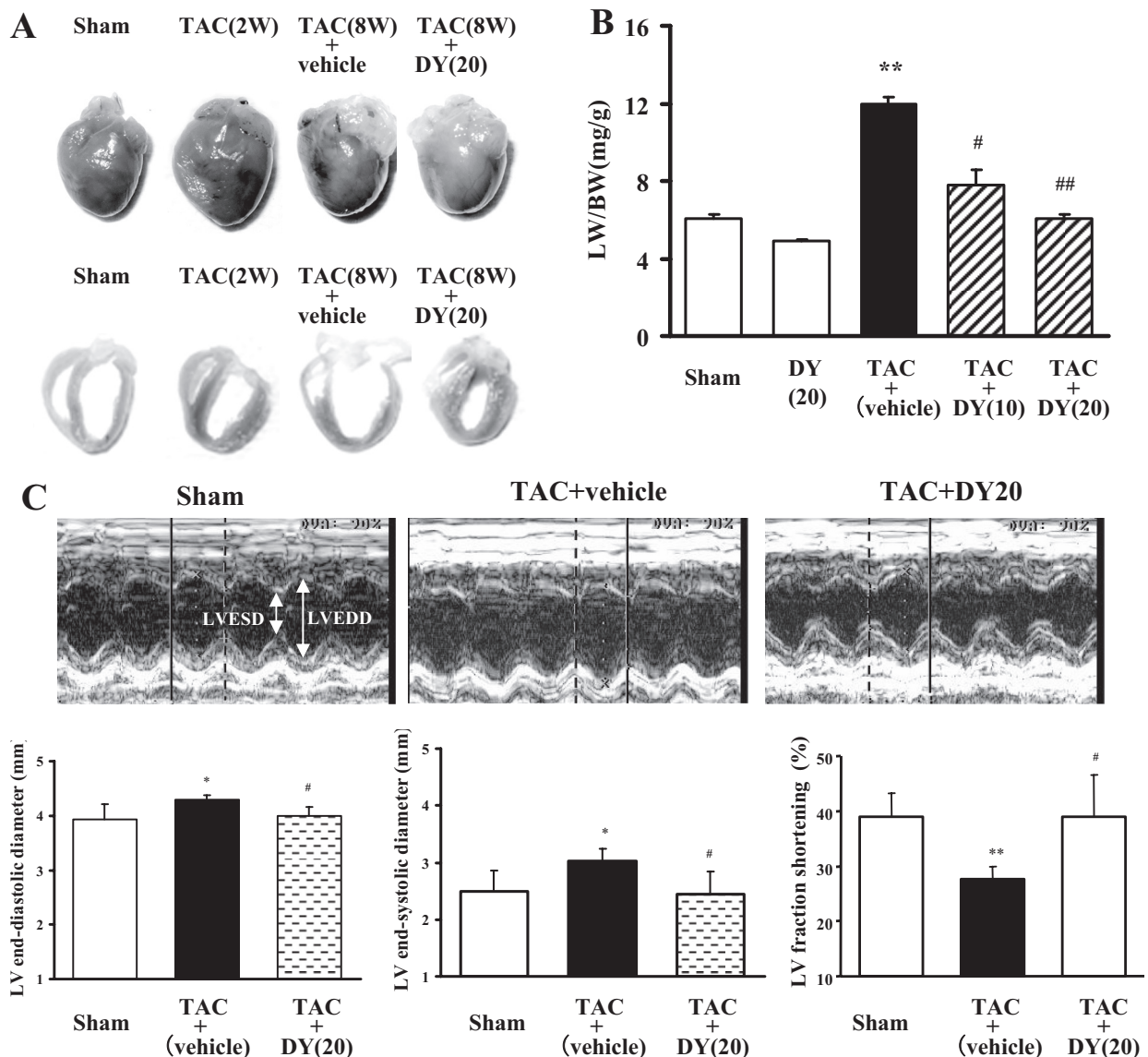


Fig. 1. DY-9760e treatment effectively inhibits pressure overload-induced cardiomyocyte hypertrophy. After 2 weeks (W) of TAC, DY-9760e [10 or 20 mg/kg (DY10 or DY20)] was orally administered daily for the next 6 weeks of TAC. A, after isolation of whole heart, the sections are fixed in paraformaldehyde solution. B, HW/BW ratio was used as an index of cardiac hypertrophy. Data are expressed as percentage of values of sham-operated animals (mean \pm S.E.M.; $n = 6$). **, $P < 0.01$ versus sham; #, $P < 0.05$; ##, $P < 0.01$ versus vehicle. C, top, representative motion-mode echocardiographic images were obtained in conscious mice 8 weeks after aortic banding with or without DY-9760e (20 mg/kg) treatment. Bottom, data are expressed as percentage of values of sham-operated animals (mean \pm S.E.M.; $n = 4$). *, $P < 0.05$ versus sham; #, $P < 0.05$ versus vehicle.

induce eNOS uncoupling and generate superoxide rather than nitric oxide. As expected, reduced levels of eNOS dimers and reciprocally increased levels of eNOS monomers were observed in LV extracts 8 weeks after TAC (Fig. 5C). DY-9760e treatment dose-dependently restored the dimeric form of eNOS, suggesting formation of physiological coupled eNOS (Fig. 5C). Likewise, peroxynitrite formation, as assessed by protein tyrosine nitration in LV extracts, was markedly increased by TAC and blocked by DY-9760e dose-dependently (Fig. 5D). Increased peroxynitrite formation suggests generation of superoxide by uncoupled eNOS, as we have shown in cultured cardiomyocytes (Lu et al., 2009a).

Discussion

Calpain activation triggers cleavage of several membrane-associated cytoskeletal proteins such as dystrophin

and spectrin. Disruption of the submembranous structure of cardiomyocytes triggered by dystrophin breakdown causes contractile dysfunction in the muscle of dystrophic patients (Toyo-oka et al., 2004). Here, we demonstrated that calpain activation upon pressure overload leads to dystrophin breakdown. In addition, disruption of eNOS localization by caveolin-3 breakdown in caveolae structures probably induces aberrant eNOS uncoupling and superoxide generation, contributing to cardiomyocyte injury and contractile dysfunction. Thus, inhibiting the calpain/dystrophin cascade and eNOS uncoupling could represent a novel therapeutic approach to inhibit heart dysfunction and heart failure. A critical finding of the present study is that DY-9760e, a novel calmodulin antagonist, effectively blocked both dystrophin breakdown and eNOS uncoupling in vivo in a mouse TAC model. DY-9760e

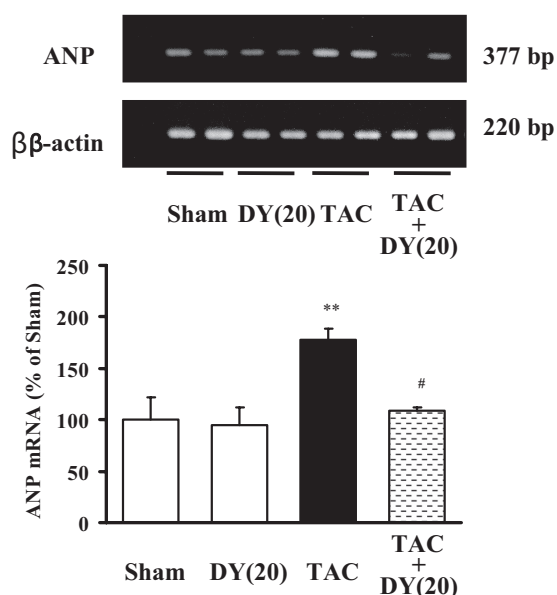


Fig. 2. DY-9760e treatment inhibits TAC-induced ANP expression. After 2 weeks of sham or TAC treatment, DY-9760e (20 mg/kg) was orally administered for 6 weeks to sham or experimental groups. Top, reverse transcription-PCR products of ANP and β -actin are shown. Bottom, quantitation of ANP and β -actin mRNA levels shown as a percentage of values of sham-operated animals (mean \pm S.E.M.; $n = 6$). **, $P < 0.01$ versus sham-operated mice; #, $P < 0.05$ versus vehicle-treated TAC mice.

protective activity was further evidenced by inhibition of spectrin breakdown and protein tyrosine nitration in the LV after TAC.

Our previous *in vitro* study demonstrated that DY-9760e inhibits ET-1-induced cardiomyocyte hypertrophy and dystrophin breakdown in cultured cardiomyocytes (Lu et al., 2007). In addition, DY-9760e significantly inhibits activation of Ca^{2+} /CaM-dependent nitric-oxide synthase after brain and heart ischemia (Hashiguchi et al., 2004; Hashimoto et al., 2005; Han et al., 2006). The antihypertrophic effect of DY9760e is mediated primarily by inhibition of Ca^{2+} /CaM-dependent activation of CaMKII δ in cardiomyocytes (Lu et al., 2009b). This pathway, together with dystrophin/spectrin breakdown and eNOS uncoupling, underlies cardiomyocyte injury after cardiac hypertrophy.

Dystrophin is essential to maintain membrane integrity in cardiac and skeletal myocytes. Its disruption in the submembranous structure triggers heart failure after cardiac hypertrophy (Toyo-Oka et al., 2004; Kawada et al., 2005). The idea that membrane dystrophin is lost to the cytosol during the early weeks after TAC was supported by immunohistochemistry after prolonged TAC. Calpains are calcium- and thiol-dependent proteases whose overactivation is implicated in several diseases, including cardiovascular disease (Matsumura et al., 1996) and ischemic stroke (Yoshida et al., 1995). Calpain activation followed by dystrophin breakdown leads to myocardial injury. Indeed, breakdown of dystrophin and spectrin correlates with myocardial injury after cardiac ischemia (Armstrong et al., 2001; Hashimoto et al., 2005). In cardiac ischemia, calpain activity mediates impaired Na^+/K^+ -ATPase activity with concomitant spectrin breakdown (Inserre et al., 2005). Because Na^+/K^+ -ATPase interacts with the cytoskeletal protein spectrin through ankyrin, spectrin breakdown probably mediates impairment of Na^+/K^+ -ATPase after cardiac ischemia. It is

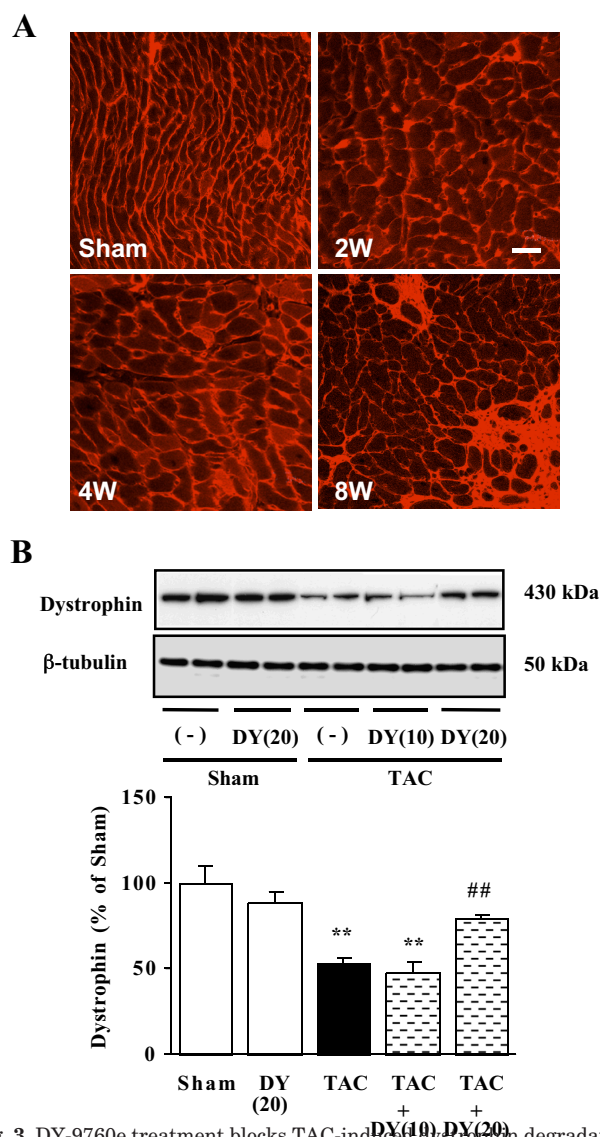


Fig. 3. DY-9760e treatment blocks TAC-induced dystrophin degradation. A, immunohistochemical localization of dystrophin in sham- and TAC-operated animals. Localization of dystrophin in the plasma membrane of cardiomyocytes indicates enlargement of cardiomyocytes 2 weeks (2W) after TAC and redistribution of dystrophin at 4 and 8 weeks after TAC. Scale bar, 40 μm . B, immunoblotting analyses of LV extracts (top) show markedly reduced levels of dystrophin 8 weeks after TAC and indicate that 6 weeks of DY-9760e treatment (20 mg/kg) began after 2 weeks of TAC significantly inhibit dystrophin breakdown. Bottom, quantitative analyses are shown in the bar graph as percentage of values of sham-operated animals (mean \pm S.E.M.; $n = 6$). **, $P < 0.01$ versus sham-operated mice; #, $P < 0.01$ versus vehicle-treated TAC mice.

interesting to note that overexpression of calpastatin, an endogenous calpain inhibitor, blunts angiotensin II-induced cardiac hypertrophy and perivascular fibrosis in heart (Letavernier et al., 2008). However, the precise mechanism underlying DY-9760e-induced inhibition of spectrin breakdown remains unclear.

Spectrin contains a calmodulin binding site, and calmodulin/ α II-spectrin interaction regulates cleavage efficacy by calpains and caspases (Rotter et al., 2004). Accumulating evidence also demonstrates that Ca^{2+} /calmodulin stimulates degradation of brain spectrin by calpain (Seubert et al., 1987; Harris et al., 1989). Thus, as a CaM antagonist, DY-9760e probably indirectly inhibits calpain-mediated

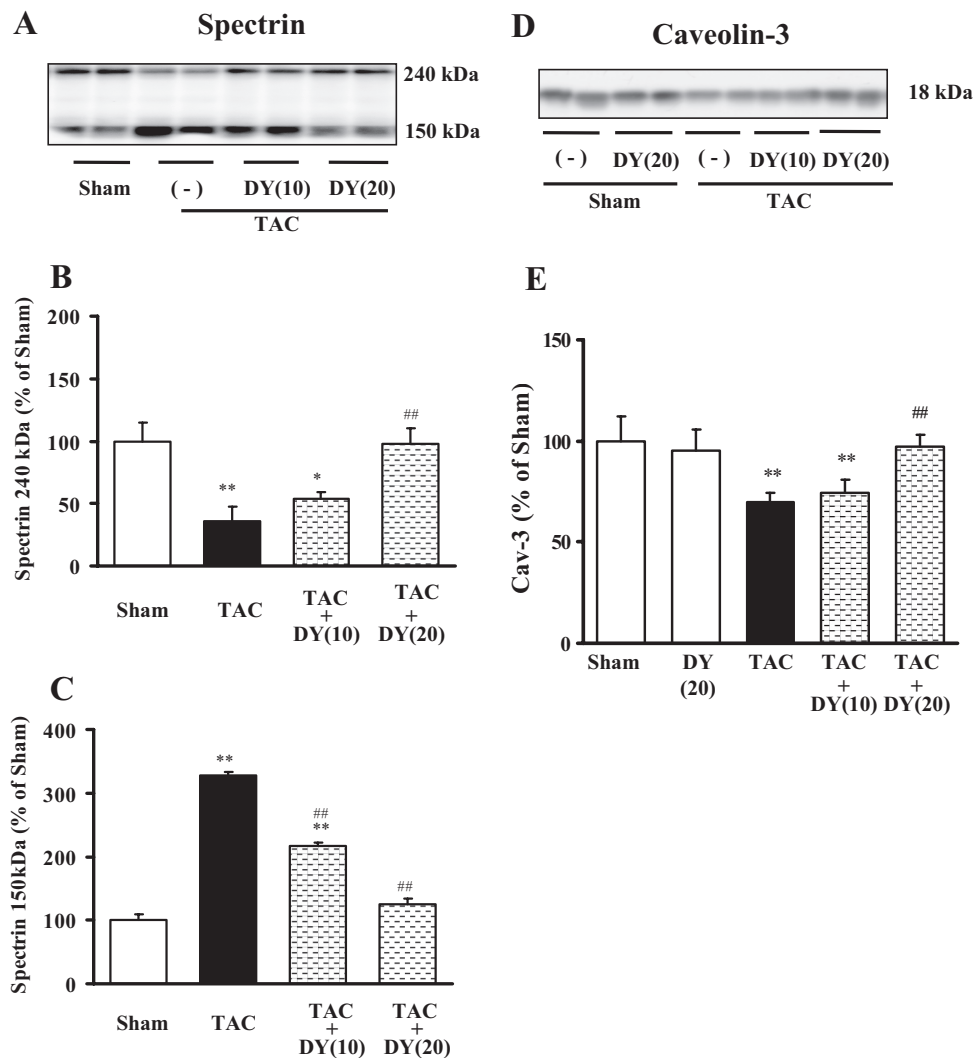


Fig. 4. DY-9760e treatment antagonizes TAC-induced spectrin and caveolin-3 breakdown. A, after 8 weeks of TAC, immunoblotting of LV extracts with anti-spectrin antibody showed that levels of 240-kDa spectrin were markedly reduced in untreated (-) animals compared with sham-operated animals. Six weeks of DY-9760e [10 and 20 mg/kg (DY10 or DY20)] treatment after 2 weeks of TAC significantly and dose-dependently inhibited TAC-induced spectrin breakdown. Inversely, the level of calpain-cleaved 150-kDa spectrin was increased by TAC and reduced by DY-9760e treatment dose-dependently. B and C, quantitative analyses of levels of 240- and 150-kDa spectrin are summarized, respectively, as a percentage of values seen in sham-operated animals (mean \pm S.E.M.; $n = 6$). D, Immunoblotting of LV extracts with an anti-caveolin-3 antibody indicates that levels of 18-kDa caveolin-3 were significantly reduced 8 weeks after TAC (-) compared with sham-operated animals. Six weeks of DY-9760e treatment (20 mg/kg) began after 2 weeks of TAC significantly inhibited TAC-induced caveolin-3 breakdown. E, quantitative analyses are presented as the percentage of values seen in sham-operated animals (mean \pm S.E.M.; $n = 6$). *, $P < 0.05$; **, $P < 0.05$ versus sham-operated mice; ##, $P < 0.01$ versus vehicle-treated TAC mice.

spectrin cleavage by inhibiting calmodulin-binding to spectrin.

DY-9760e cardioprotection also includes protection of eNOS/caveolin-3 signaling in caveolae. In cardiac myocytes, the eNOS isoform mostly localizes in caveolae where it associates with caveolin-3 (García-Cardena et al., 1996; Feron et al., 1996). Caveolin-3 inhibits eNOS activity, whereas calmodulin binding to eNOS after Ca^{2+} mobilization disrupts caveolin-3 binding, leading to eNOS activation and nitric oxide production (Michel and Feron, 1997). Our previous study documented that dystrophin breakdown was closely associated with translocation of caveolin-3 from caveolae and decreased Ca^{2+} /CaM-dependent nitric oxide generation by eNOS in cultured cardiomyocytes (Lu et al., 2009a). Likewise, dystrophin knockout mice show impaired nitric oxide-dependent and endothelium-dependent vasodilation in arteries (Loufrani et al., 2004). In the present study, we demonstrated in vivo that disruption of eNOS association with caveolin-3 is associated with eNOS uncoupling, thereby increasing peroxynitrite formation, as assessed by protein tyrosine nitration. Indeed, superoxide generation is closely associated with eNOS uncoupling in cultured cardiomyocytes exposed to phenylephrine (Lu et al., 2009a). Furthermore, treatment with DY-9836, an active metabolite of

DY-9760e, largely inhibited elevation both of superoxide and nitric oxide generation after prolonged exposure to phenylephrine in cultured cardiomyocytes. Under the same conditions, generation of monomeric eNOS was also inhibited by DY-9836 treatment (Lu et al., 2009a). It is noteworthy that Tempol (a radical scavenger), DY-9836, and N^G -nitro-L-arginine methyl ester (a NO synthase inhibitor) all completely inhibited apoptosis of cardiomyocytes exposed to phenylephrine (Lu et al., 2009a).

Accumulating evidence confirms the pathophysiological relevance of eNOS uncoupling and peroxynitrite generation to TAC-induced heart failure. Tetrahydrobiopterin (BH4) treatment in TAC-induced hypertrophy inhibited pressure overload-induced oxidative stress through reversal of eNOS uncoupling, thereby ameliorating cardiac hypertrophy/dysfunction in mice (Takimoto et al., 2005; Moens et al., 2008). The reversal of eNOS uncoupling by exogenous BH4 was more effective than Tempol in preventing heart failure (Moens et al., 2008). Likewise, infusion of peroxynitrite or a peroxynitrite donor such as 3-morpholino sydnonimine impaired contractile function by altering Ca^{2+} handling and/or β -adrenergic responsiveness in isolated myocytes (Katori et al., 2006; Kohr et al., 2008). Taken together, in addition to dystrophin/spectrin breakdown, de-

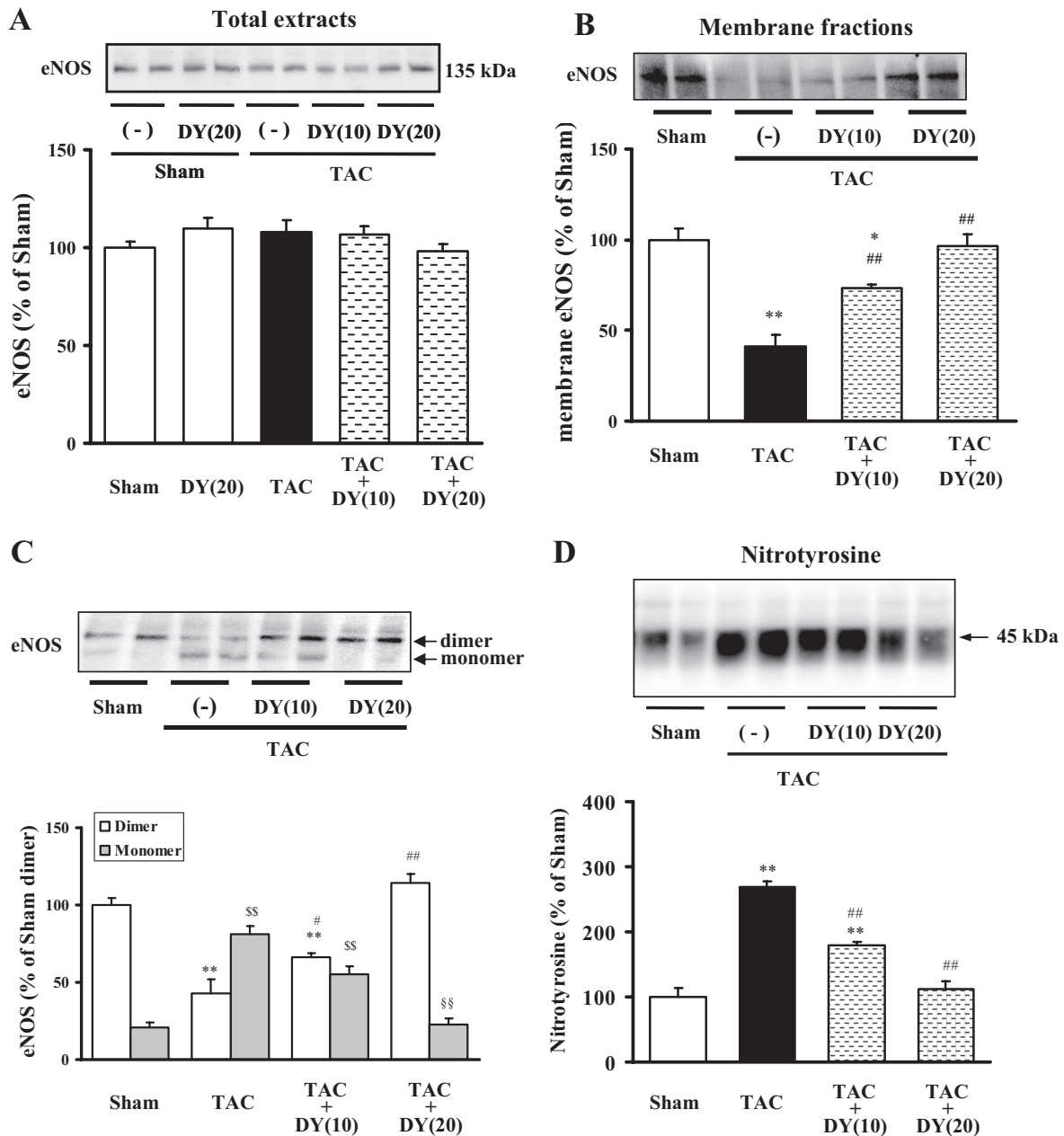


Fig. 5. Effects of DY-9760e on TAC-induced membrane eNOS levels, eNOS uncoupling, and nitrotyrosine formation. A, representative image (top) and bar graph (bottom) showing results of immunoblotting of total heart extracts with anti-eNOS antibody. Analysis indicates no apparent changes in total eNOS levels among conditions. B, representative image (top) and bar graph (bottom) showing results of immunoblotting with anti-eNOS antibody. Analysis of cell membrane extracts indicates marked reduction in eNOS levels in TAC animals and rescue of eNOS levels after DY-9760e treatment dose-dependently. Data are expressed as a percentage of values seen in sham-operated animals (mean \pm S.E.M.; $n = 6$). *, $P < 0.05$; **, $P < 0.01$ versus sham-operated mice; ##, $P < 0.01$ versus vehicle-treated mice. C, levels of uncoupled (monomer) eNOS are shown as analyzed by low-temperature SDS-polyacrylamide gel electrophoresis (top). Quantitation of dimeric and monomeric eNOS (lower) was performed by densitometric analysis. Dimeric eNOS from sham-operated animals was arbitrarily set at 100%. Data are expressed as percentage of values seen in sham-operated animals (mean \pm S.E.M.; $n = 6$). **, $P < 0.01$ versus sham-operated mice (dimer); #, $P < 0.05$ and ##, $P < 0.01$ versus vehicle-treated mice (dimer); \$\$, $P < 0.01$ versus sham-operated mice (monomer); and \$\$\$, $P < 0.01$ versus vehicle-treated mice (monomer). D, representative image (top) and bar graph (bottom) of immunoblots of total heart extracts with anti-nitrotyrosine antibody. Analysis indicates that protein tyrosine nitration was markedly increased after TAC compared with sham-operated animals and decreased by DY-9760e treatment dose-dependently. **, $P < 0.01$ versus sham-operated mice; ##, $P < 0.01$ versus vehicle-treated TAC mice.

creased BH4 levels in cardiomyocytes probably underlies eNOS uncoupling, leading to heart failure by oxidant stress, including peroxynitrite generation.

In summary, we report that a CaM antagonist, DY-9760e, inhibits in vivo the progression of cardiac hypertrophy-induced cardiac injury by inhibiting calpain-mediated dystrophin/spectrin degeneration and loss of caveolae integrity in cardiomyo-

cyte plasma membranes (Fig. 6). Protein tyrosine nitration through superoxide generation by uncoupled eNOS was also ameliorated by DY-9760e treatment. Loss of caveolae integrity probably triggers eNOS uncoupling by dissociation from the plasma membranes. Taken together, evidence gathered using the TAC mouse model is consistent with our previous results obtained in cultured cardiomyocytes, supporting the idea that

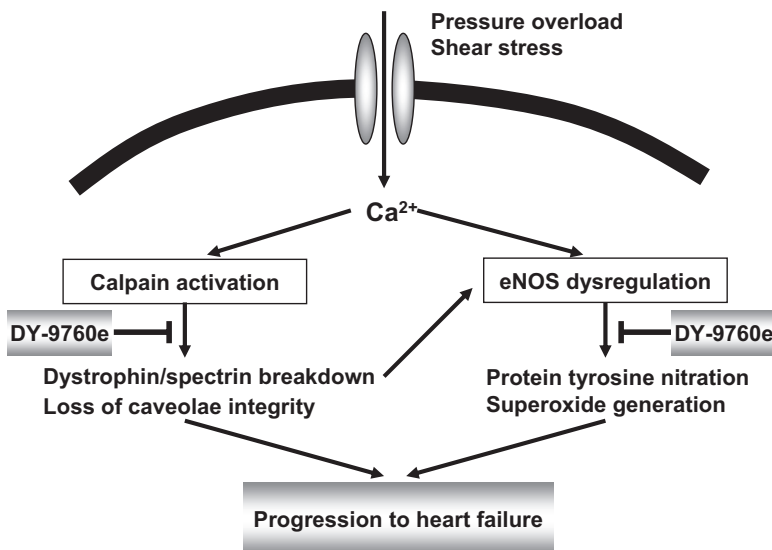


Fig. 6. Potential cardioprotective mechanism of DY-9760 on TAC-induced heart injury. DY-9760e in vivo inhibits progression of cardiac hypertrophy-induced cardiac injury by inhibiting calpain-mediated dystrophin/spectrin degeneration and loss of caveolae integrity in cardiomyocyte plasma membranes. Protein tyrosine nitration through superoxide generation by uncoupled eNOS is also ameliorated by DY-9760e treatment. Loss of caveolae integrity probably triggers eNOS uncoupling by dissociation from plasma membranes.

DY-9760e treatment could provide a novel therapeutic strategy to treat hypertrophy and heart failure.

References

- Armstrong SC, Latham CA, Shivel CL, and Ganote CE (2001) Ischemic loss of sarcolemmal dystrophin and spectrin: correlation with myocardial injury. *J Mol Cell Cardiol* **33**:1165–1179.
- Brown DW, Giles WH, and Croft JB (2000) Left ventricular hypertrophy as a predictor of coronary heart disease mortality and the effect of hypertension. *Am Heart J* **140**:848–856.
- Feron O, Belhassen L, Kobzik L, Smith TW, Kelly RA, and Michel T (1996) Endothelial nitric oxide synthase targeting to caveolae. Specific interactions with caveolin isoforms in cardiac myocytes and endothelial cells. *J Biol Chem* **271**:22810–22814.
- García-Cardena G, Oh P, Liu J, Schnitzer JE, and Sessa WC (1996) Targeting of nitric oxide synthase to endothelial cell caveolae via palmitoylation: implications for nitric oxide signaling. *Proc Natl Acad Sci U S A* **93**:6448–6453.
- Haider AW, Larson MG, Benjamin EJ, and Levy D (1998) Increased left ventricular mass and hypertrophy are associated with increased risk for sudden death. *J Am Coll Cardiol* **32**:1454–1459.
- Han F, Shirasaki Y, and Fukunaga K (2006) Microsphere embolism-induced endothelial nitric oxide synthase expression mediates disruption of the blood-brain barrier in rat brain. *J Neurochem* **99**:97–106.
- Harris AS, Croall DE, and Morrow JS (1989) Calmodulin regulates fodrin susceptibility to cleavage by calcium-dependent protease I. *J Biol Chem* **264**:17401–17408.
- Hashiguchi A, Yano S, Morioka M, Hamada J, Shirasaki Y, Kochi M, and Fukunaga K (2004) The post-ischemic administration of 3-[2-[4-(3-chloro-2-methylphenyl)-1-piperazinyl]ethyl]-5,6-dimethoxy-1-(4-imidazolylmethyl)-1H-indazole dihydrochloride 3.5 hydrate (DY-9760e), a novel calmodulin antagonist, prevents delayed neuronal death in gerbil hippocampus. *J Pharmacol Sci* **96**:65–72.
- Hashimoto M, Takada Y, Takeuchi Y, Kasahara J, Hira H, Shirasaki Y, and Fukunaga K (2005) Cytoprotective effect of 3-[2-[4-(3-chloro-2-methylphenyl)-1-piperazinyl]ethyl]-5,6-dimethoxy-1-(4-imidazolylmethyl)-1H-indazole dihydrochloride 3.5 hydrate (DY-9760e) against ischemia/reperfusion-induced injury in rat heart involves inhibition of fodrin breakdown and protein tyrosine nitration. *J Pharmacol Sci* **98**:142–150.
- Hu P, Zhang D, Swenson L, Chakrabarti G, Abel ED, and Litwin SE (2003) Minimally invasive aortic banding in mice: effects of altered cardiomyocyte insulin signaling during pressure overload. *Am J Physiol Heart Circ Physiol* **285**:H1261–H1269.
- Inserte J, Garcia-Dorado D, Hernandez V, and Soler-Soler J (2005) Calpain-mediated impairment of Na⁺/K⁺-ATPase activity during early reperfusion contributes to cell death after myocardial ischemia. *Circ Res* **97**:465–473.
- Jugdutt BI (2003) Remodeling of the myocardium and potential targets in the collagen degradation and synthesis pathways. *Curr Drug Targets Cardiovasc Haematol Disord* **3**:1–30.
- Katori T, Donzelli S, Tocchetti CG, Miranda KM, Cormaci G, Thomas DD, Ketner EA, Lee MJ, Mancardi D, Wink DA, et al. (2006) Peroxynitrite and myocardial contractility: in vivo versus in vitro effects. *Free Radic Biol Med* **41**:1606–1618.
- Kawada T, Masui F, Kumagai H, Koshimizu M, Nakazawa M, and Toyo-Oka T (2005) A novel paradigm for therapeutic basis of advanced heart failure—assessment by gene therapy. *Pharmacol Ther* **107**:31–43.
- Kohr MJ, Wang H, Wheeler DG, Velayutham M, Zweier JL, and Ziolo MT (2008) Biphasic effect of SIN-1 is reliant upon cardiomyocyte contractile state. *Free Radic Biol Med* **45**:73–80.
- Levy D, Larson MG, Vasan RS, Kannel WB, and Ho KK (1996) The progression from hypertension to congestive heart failure. *Jama* **275**:1557–1562.
- Letavernier E, Perez J, Bellocq A, Mesnard L, de Castro Keller A, Haymann JP, and Baud L (2008) Targeting the calpain/calpastatin system as a new strategy to prevent cardiovascular remodeling in angiotensin II-induced hypertension. *Circ Res* **102**:720–728.

- Loufrani L, Dubroca C, You D, Li Z, Levy B, Paulin D, and Henrion D (2004) Absence of dystrophin in mice reduces NO-dependent vascular function and vascular density: total recovery after a treatment with the aminoglycoside gentamicin. *Arterioscler Thromb Vasc Biol* **24**:671–676.
- Lu YM, Han F, Shioda N, Moriguchi S, Shirasaki Y, Qin ZH, and Fukunaga K (2009a) Phenylephrine-induced cardiomyocyte injury is triggered by superoxide generation through uncoupled endothelial nitric-oxide synthase and ameliorated by 3-[2-[4-(3-chloro-2-methylphenyl)-1-piperazinyl]ethyl]-5,6-dimethoxyindazole (DY-9836), a novel calmodulin antagonist. *Mol Pharmacol* **75**:101–112.
- Lu YM, Shioda N, Han F, Kamata A, Shirasaki Y, Qin ZH, and Fukunaga K (2009b) DY-9760e inhibits endothelin-1-induced cardiomyocyte hypertrophy through inhibition of CaMKII and ERK activities. *Cardiovasc Ther* **27**:17–27.
- Lu YM, Shioda N, Han F, Moriguchi S, Kasahara J, Shirasaki Y, Qin ZH, and Fukunaga K (2007) Imbalance between CaM kinase II and calcineurin activities impairs caffeine-induced calcium release in hypertrophic cardiomyocytes. *Biochem Pharmacol* **74**:1727–1737.
- Matsumura Y, Saeki E, Inoue M, Hori M, Kamada T, and Kusuoka H (1996) Inhomogeneous disappearance of myofilament-related cytoskeletal proteins in stunned myocardium of guinea pig. *Circ Res* **79**:447–454.
- Meijs MF, de Windt LJ, de Jonge N, Cramer MJ, Bots ML, Mali WP, and Doevendans PA (2007) Left ventricular hypertrophy: a shift in paradigm. *Curr Med Chem* **14**:157–171.
- Michel T and Feron O (1997) Nitric oxide synthases: which, where, how, and why? *J Clin Invest* **100**:2146–2152.
- Moens AL, Takimoto E, Tocchetti CG, Chakir K, Bedja D, Cormaci G, Ketner EA, Majmudar M, Gabrielson K, Halushka MK, et al. (2008) Reversal of cardiac hypertrophy and fibrosis from pressure overload by tetrahydrobiopterin: efficacy of recoupling nitric oxide synthase as a therapeutic strategy. *Circulation* **117**:2626–2636.
- Rotter B, Kroviarski Y, Nicolas G, Dhermy D, and Lecomte MC (2004) AlphaII-spectrin is an in vitro target for caspase-2, and its cleavage is regulated by calmodulin binding. *Biochem J* **378**:161–168.
- Saido TC, Sorimachi H, and Suzuki K (1994) Calpain: new perspectives in molecular diversity and physiological-pathological involvement. *FASEB J* **8**:814–822.
- Seubert P, Baudry M, Dudek S, and Lynch G (1987) Calmodulin stimulates the degradation of brain spectrin by calpain. *Synapse* **1**:20–24.
- Spinale FG (2007) Myocardial matrix remodeling and the matrix metalloproteinases: influence on cardiac form and function. *Physiol Rev* **87**:1285–1342.
- Takimoto E, Champion HC, Li M, Ren S, Rodriguez ER, Tavazzi B, Lazzarino G, Paolucci N, Gabrielson KL, Wang Y, et al. (2005) Oxidant stress from nitric oxide synthase-3 uncoupling stimulates cardiac pathologic remodeling from chronic pressure load. *J Clin Invest* **115**:1221–1231.
- Toyo-Oka T, Kawada T, Nakata J, Xie H, Urabe M, Masui F, Ebisawa T, Tezuka A, Iwasawa K, Nakajima T, et al. (2004) Translocation and cleavage of myocardial dystrophin as a common pathway to advanced heart failure: a scheme for the progression of cardiac dysfunction. *Proc Natl Acad Sci U S A* **101**:7381–7385.
- Weber KT (1989) Cardiac interstitium in health and disease: the fibrillar collagen network. *J Am Coll Cardiol* **13**:1637–1652.
- Yoshida H, Takahashi M, Koshimizu M, Tanonaka K, Oikawa R, Toyo-oka T, and Takeo S (2003) Decrease in sarcoglycans and dystrophin in failing heart following acute myocardial infarction. *Cardiovasc Res* **59**:419–427.
- Yoshida K, Inui M, Harada K, Saido TC, Sorimachi Y, Ishihara T, Kawashima S, and Sobue K (1995) Reperfusion of rat heart after brief ischemia induces proteolysis of caldesmon (nonerythroid spectrin or fodrin) by calpain. *Circ Res* **77**:603–610.

Address correspondence to: Dr. Kohji Fukunaga, Department of Pharmacology, Graduate School of Pharmaceutical Sciences, Tohoku University, Aramaki-Aoba Aoba-ku, Sendai 980-8578, Japan. E-mail: fukunaga@mail.pharm.tohoku.ac.jp